Plasmonic Fabry-Pérot Nanocavity

Volker J. Sorger,[†,§] Rupert F. Oulton,[†,§] Jie Yao,[†] Guy Bartal,[†] and Xiang Zhang*,[†,‡]

NSF Nanoscale Science and Engineering Centre, 3112 Etcheverry Hall, University of California, Berkeley, California, 94720, and Materials Sciences Division, Lawrence Berkeley National Laboratory, 1 Cyclotron Road, Berkeley, California 94720

ABSTRACT

We experimentally demonstrate a novel, all-plasmonic nanoscopic cavity exhibiting Q-factors up to 200 at visible frequencies. The Fabry-Pérot type resonator uses tall metallic fins that reflect up to 98% of incident surface plasmon to concentrate light within a subwavelength cavity mode. High aspect ratio metal fins, constructed using lithography and electroplating, reduce surface plasmon scattering out of the surface, while a short cavity length reduces the propagation loss. A simple Fabry-Pérot cavity model adapted for surface plasmon dispersion and reflection describes the underlying physics of the nanocavities and the results agree well with Johnson's and Christie's permittivity data. The occurrence of an optimum wavelength for plasmon storage in these cavities allows us to clearly visualize the fundamental trade-off between propagation loss and the spatial extent of surface plasmon polaritons. The subwavelength optical mode area within these cavities enables the enhancement of weak optical processes such as spontaneous emission and nonlinear optics at nanoscale dimensions.

Scaling photonic devices beyond the diffraction limit of light imposes a fundamental challenge and is expected to introduce a range of new and enhanced physical effects. Surface plasmons,[1] collective oscillations of free electrons, show the potential to overcome this limitation enabling nanophotonic applications such as nanoscale waveguides,[2,3] Bragg mirrors,[4] interferometers and ring-resonators,[5] single plasmon generation,[6] and cavities.[7] Nonplasmonic microcavities such as vertical cavity surface emitting lasers,[8] microring resonators,[9] and photonic crystals[10] have microscale dimensions with mode volumes at the order of or larger than the wavelength of light. Plasmonic cavities on the other hand can be truly nanoscale with mode dimensions way below the wavelength of the light.[7] However, the intrinsic losses associated with SPPs are generally known to limit plasmonic device performance (for example, reducing the quality factor). Beyond technological incentives, accessing optical length scales well below the diffraction limit allows the enhancement of weak physical processes by orders of magnitude.[6,11–17]

Optical cavities allow efficient concentration and storage of electromagnetic energy and are consequently used throughout optics for numerous light emission and detection applications.[9] However, in order to enhance the aforementioned physical processes, it is essential to concentrate light in a small mode volume and store it there for a long time. The cavity quality factor, Q, is a measure of the time that light is trapped inside a cavity and is determined by the optical feedback mechanism (e.g., mirror reflectivity) and the internal loss. While the Q-factors of conventional dielectric cavities can be quite high,[8–10] they exhibit relatively weak optical confinement with modal volumes generally larger than the wavelength cubed. Plasmonic cavities on the other hand, can achieve strong mode confinement, but possess intrinsic SPP and scattering losses that in general, reduce the cavity Q-factor well below its dielectric counterpart.[7,18–20]

Here we demonstrate a plasmonic Fabry-Pérot nanocavity with a Q-factor close to 200. This is obtained by a novel design of closely spaced high-aspect ratio mirrors, capable of reflecting up to 98% of incident SPPs. Since the cavity length is much shorter than the SPP propagation distance and the mirrors' heights are significantly larger than the SPP penetration depth in air, the loss per round trip and mirror scattering are minimized, respectively. In fact, the SPP propagation loss in these nanocavities accounts for only a small reduction in the quality factor.

The nanocavity is made of two parallel silver fins acting as high quality optical mirrors standing perpendicular to a silver film (Figure 1a). Standard electron beam lithography was used to write the nanocavity pattern into 1.1 μm thick poly(methyl methacrylate) (PMMA) layer on top a 200 nm thick silver film on a Si substrate. The cavity mirrors were grown via chemically electroplating silver (80 pA for 70 s) followed by final PMMA lift off in acetone. A post fabrication rapid thermal annealing step in nitrogen at 400 C for 60 s helps to smooth the metal surfaces. While the back mirror, $L_b = 250$ nm, is 10 times the skin depth of

---

* To whom correspondence should be addressed. E-mail: xiang@berkeley.edu.
† University of California.
‡ Lawrence Berkeley National Laboratory.
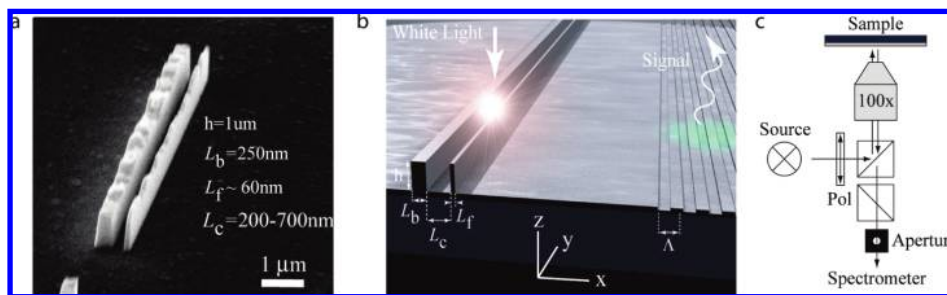§ These authors contributed equally to this work.

Figure 1. The plasmonic Fabry-Pérot nanocavity. (a) Tilted scanning electron micrograph of a nanocavity. Vertical silver fins act as mirrors for SPPs bound to the underlying silver–air interface. SPP cavity modes were coupled out by the tall-and-thin front mirror (20:1 aspect ratio). (b,c) Schematics of the nanocavity and the optical characterization method. White light (Xe lamp 150W, polarized along x-direction) was focused through a $100\times$ with NA = 0.9 microscope objective onto the nanocavity, exciting SPP cavity modes. The SPP signal was scattered out of the plane by a grating coupler (10 grooves, 10 μm long, pitch 247 nm) situated 20 μm from the cavity. A 2 μm aperture defines a collection region on the grating and the signal was sent to a N_2-cooled spectrometer/CCD. High signal-to-noise ratios were obtained by placing an aperture in a secondary image plane. A second polarizer ensured that only waves originating in SPPs are detected at the grating coupler. T = 300 K.

silver, the front mirror must be sufficiently thin ($L_f = 55-85$ nm) to allow partial out-coupling of resonant surface plasmons in the forward direction. This imposes the requirement of a high aspect ratio (20:1) mirror that cannot be obtained by fabrication techniques such as evaporation or sputtering due to their nondirectional nature. While reactive ion etching can lead to structures with a high aspect ratio, it has been found to produce rough surfaces for noble metals such as silver.[21] A top-down RIE etched nanocavity with the same design would result not only in rough cavity mirrors, but also in a rough bottom silver film. We found that a combination of high resolution lithography and electrochemical metal deposition yielded the required high aspect ratio. Since the SPP mode of the cavity is propagating along this film, any roughness directly reduces the SPP propagation length due to increased scattering into the far field, hence lowering the Q-factor of a cavity.[1] Devices shown in this report had a surface roughness of about 1.03 nm (Supporting Information).

Excitation of the nanocavity can be achieved by focusing white light onto the mirrors, which scatter the light into the various optical modes of the nanocavity (Figure 1b). The SPP nanocavity modes are transmitted through the thin front mirror and scattered into free-space by a FIB milled broadband grating coupler, situated 20 μm from the cavity (10 grooves: 10 μm long (y-direction), pitch = 247 nm, depth = 45 nm, Figure 1b,c). We have estimated that the front mirror transmits between 1 and 2% of incident light per round trip based on numerical simulations (see Supporting Information). Light from the grating is then detected through an aperture that defines a 2 μm collection region on the grating. In this way, we can effectively spatially filter cavity modes at oblique incidence to the mirrors.[21] Figure 2a depicts the spectra collected from the grating coupler for 7 selected of the 14 measured (for clarity) nanocavities with lengths, L_c, ranging from 175 to 700 nm. A sharp resonance that is indicative of a high Q-factor mode is observable for each nanocavity. Aside from the sharp peak, whose spectral position depends on the cavity length, L_c, a weaker and broader background hump is also apparent, which is spectrally similar for all the cavities (Supporting Information).
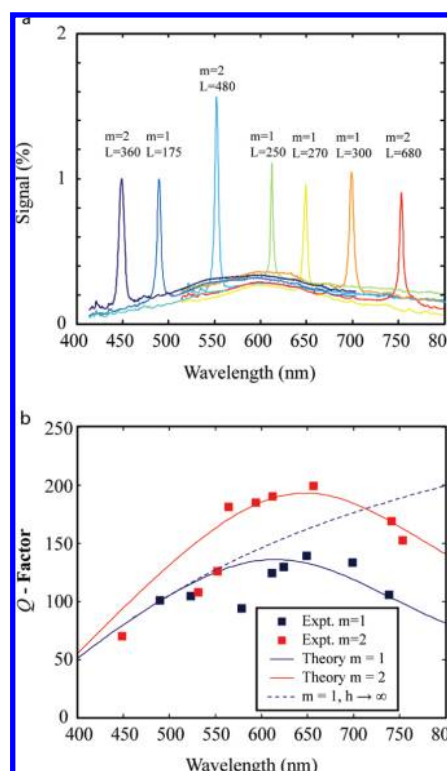

Figure 2. Spectral response and Q-factors of Fabry-Pérot nanocavities of varying length. (a) Relative signal intensity ($\sim$1% of the excitation intensity) for 7 selected cavity lengths (175–700 nm) of the 14 measured (for clarity) spanning the visible spectrum. Each cavity length has a single, sharp resonance corresponding to horizontal oscillation between metal mirrors (H-mode). (b) Q-factors measured for the first and second order cavity modes (square markers). Theoretical trend lines (solid) highlight the competition between intrinsic metal and scattering losses. For $h \rightarrow \infty$, Q-factors are primarily affected by metallic losses (dashed line) which increase for shorter wavelengths. Conversely, scattering loss dominates at longer wavelengths due to the larger SPP field extension into the air, which becomes comparable with the finite fin height.

The experimentally measured Q-factors ranging from 100–200 are high for plasmonic resonators at these frequencies (Figure 2b). In fact, the plasmonic losses reduce the Q-factor by less than a half compared to that of a lossless dielectric cavity

of the same size. This is in sharp contrast to microdisks cavities with a Q-factor reduction from 10^9 in dielectric[9] to $\sim$1300 in plasmonic cavities at IR frequencies,[18] which are limited entirely by propagation loss.

In order to examine the underlying physics of these nanocavities, a Fabry-Pérot cavity model was adapted to account for SPP dispersion and reflection from the metal fins and compared with the experimental results in Figure 2a.[23] The SPP reflection at the mirrors was approximated to the Fresnel coefficient, $r(\lambda) = (n_{Ag}(\lambda) - n_{sp}(\lambda))[n_{Ag}(\lambda) + n_{sp}(\lambda)]^{-1}$, where $n_{Ag}(\lambda)$ is the refractive index of silver and $n_{sp}(\lambda)$ is the effective index of SPPs. Both the magnitude, $|r(\lambda)|$ and phase, ϕ, of the reflection coefficient, $r(\lambda) = |r(\lambda)|\exp\{i\phi(\lambda)\}$, are relevant to the physics of the nanocavity. The phase describes the shift of resonance wavelength from a perfect metal reflector due to field penetration, $\delta(\lambda)$, into the metal mirrors, which will be discussed below, where $\delta(\lambda) = -\phi(\lambda)\lambda[4\pi\mathrm{Re}\{n_{sp}(\lambda)\}]^{-1}$. The physical cavity length, L, and optical cavity length, $L_c(\lambda)$, are related such that $L_c(\lambda) = L + 2\delta(\lambda)$. $|r(\lambda)|^2$ approximates the reflectivity in the absence of scattering due to the nonzero SPP field at the upper corners of the mirrors. Assuming that the amount of scattering is small (see Supporting Information), it will be approximately proportional to the electric field intensity at the top corner of the mirror, that is, at a height, h, above the metal surface. In this case the magnitude of the reflection from the metal mirror is modeled by $R(\lambda) = |r(\lambda)|^2 - S_0 \exp(-h/L_z(\lambda))$ where $L_z(\lambda) = \lambda\mathrm{Im}\{[1 - n_{sp}(\lambda)^2]^{-1/2}\}/4\pi$ is the SPP penetration depth in air and S_0 a phenomenological constant describing the scattering strength. By incorporating the physics of surface plasmon propagation, attenuation, and scattering from the mirrors, the Q-factor of the nanocavity mode at a resonance frequency, $\lambda_R = 2\mathrm{Re}\{n_{sp}(\lambda_R)\}L_c(\lambda_R)$, is modeled using the usual Fabry-Pérot expression

$$Q(\lambda_R) = m\pi \frac{\sqrt{R(\lambda_R)}\exp(-2L_c(\lambda_R)/L_{sp}(\lambda_R))}{1 - R(\lambda_R)\exp(-2L_c(\lambda_R)/L_{sp}(\lambda_R))} \qquad (1)$$

where m is the order of the cavity mode. This nanocavity model has 4 unknowns, the Drude parameters of silver, ε_b, E_{pAg}, and γ_{Ag}, and the mirror scattering strength, S_0. Here, we have chosen $\varepsilon_b = 5$[24] and $E_{pAg} = 9.5$ eV was determined from the best fit to the cavity mode dispersion, $\lambda_R = 2\mathrm{Re}\{n_{sp}(\lambda_R)\}L_c(\lambda_R)$. The two remaining parameters are related to the observed cavity Q-factor and describe propagation loss, $\gamma_{Ag} = 0.04$ eV, and scattering loss, $S_0 = 0.37$. While S_0 is a phenomenological constant, it produces a good numerical fit to the Q-factors observed in the experiment. The three parameters that define the Drude model describe all characteristics of the nanocavity's modes well. Out of the two widely used permittivity data sets,[24,25] our results show best agreement with Johnson et al., that is, $E_{pAg} = 9.323$ eV and $\gamma_{Ag} = 0.024$ eV.[24] While the data of Johnson et al. give a propagation length about 1.6 times the observed value, Palik's data give a value that is just 38%.[25]

The theoretical model of the Fabry-Pérot nanocavity describes the trends of the Q-factors well for the first and second order cavity modes. The distinctive shape of these trend lines arises from the trade-off between the two cavity loss mechanisms, intrinsic metallic and scattering losses. The Q-factors of cavities resonating at shorter wavelengths are mainly dominated by intrinsic metallic losses including the SPP propagation distance and field penetration into the metallic mirrors. In fact, the Q-factor is not affected at all by the finite height of the mirrors since the field is tightly confined to the metal substrate (Figure 2b). Conversely, at longer wavelengths, the plasmonic mode extends further from the metal substrate into the air; hence the Q-factor is clamped by scattering losses from the upper corners of the mirrors (Figure 2b).

The measured resonant wavelengths follow the theoretical condition describing surface plasmons resonating in a horizontal (H) fashion between the metallic mirrors (Figure 3a). The observed cavity dispersion deviates from that of free space radiation bouncing between two metal mirrors since the SPP wavelength becomes increasingly shorter than that of free space at higher frequencies. The small cavity size leads to a large free spectral range, so that for each cavity length only one of two possible H-mode orders are observable (blue line = first, red line = second H-mode) in our measurements. A finite element method simulation for a cavity length of $L = 325$ nm shows two possible H-modes of the nanocavity, which lie at opposite ends of the visible spectrum (Figure 3b,c). The H-modes have plasmonic character since they are confined in the z-direction with the characteristic exponential decay and are diffraction-limited in the x-direction. The first order mode occurs at the red end of the spectrum and clearly shows penetration into air where scattering from the top of each mirror is appreciable. On the other hand, the second order mode occurs at the blue end of the spectrum where plasmonic confinement is strong and cavity loss is dominated by the SP propagation loss and field penetration into the metallic fins.

When illuminated by a finite beam spot, the nanocavity effectively contains a 3D confined mode. An estimation of the nanocavity's mode volume for a diffraction limited spot yields values between 0.24 $(\lambda/2)^3$ and 0.37 $(\lambda/2)^3$ across the visible spectrum, clearly below the diffraction limit (see Supporting Information). Metal fin reflectors can also be used to realize a 3D confined cavity mode using two approaches. First, the metal mirrors could be used in both of the plasmonic degrees of freedom, defining a metallic hole in which surface plasmons can resonate. Alternatively, 3D modal confinement can be further increased by utilizing the metallic fin reflectors to concentrate the modes of a plasmonic waveguide, for example, channel plasmon polaritons in metal grooves, as suggested by Pile and co-workers.[5a]

Using the Fabry-Pérot model from above, the cavity's feedback mechanism can be revealed by extracting the properties of the metallic mirrors; the complex reflection coefficient and the scattering from the top corners of the mirrors. The phase change upon reflection causes a small wavelength dependent shift corresponding to the finite penetration depth of SPPs into the metal mirrors, which we have determined by comparing the resonance wavelength and physical length of each cavity (Figure 4a). The measured
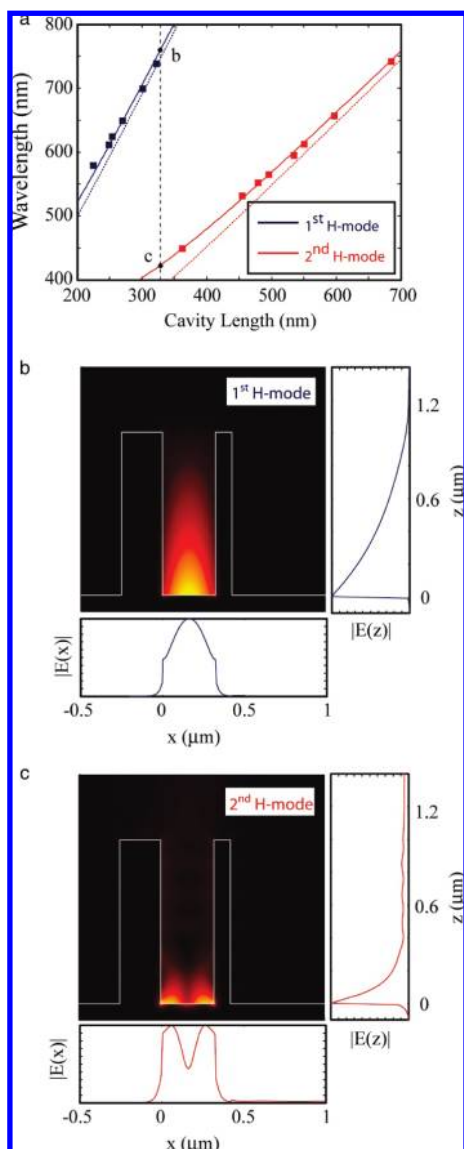
Figure 3. Dispersion and field distributions of the nanocavity modes. (a) The measured resonant wavelengths versus cavity length for the 1st and 2nd H-modes (square markers) compared with a SPP and dielectric Fabry-Pérot cavity model (solid and dotted lines), respectively. The plasmonic character of the resonance condition of the cavity can be seen from the deviation to a dielectric cavity. (b,c) |E|-field distributions of the 1st and 2nd nanocavity modes. The plasmonic character of the modes is evident from the exponential decay along the z-direction.

penetration depths closely follow the theoretical trend calculated from the reflection phase of the Fresnel coefficient. The reflectivity of the mirrors is determined from the Fabry-Pérot model and was found to be as high as 98% (Figure 4b). This measurement is the geometric average of the two mirror reflectivities, which are different due to light leakage though the thinner front mirror. The high reflectivity proves the feasibility of tall metal fins acting as efficient SPP reflectors forming a cavity. While an SPP scattering free scheme has recently been proposed utilizing anisotropic metamaterials,[26] such an approach where the dielectric permittivity needs to be controlled in at least two dimensions of the material are difficult to achieve and have yet to be demonstrated to eliminate SPP scattering.
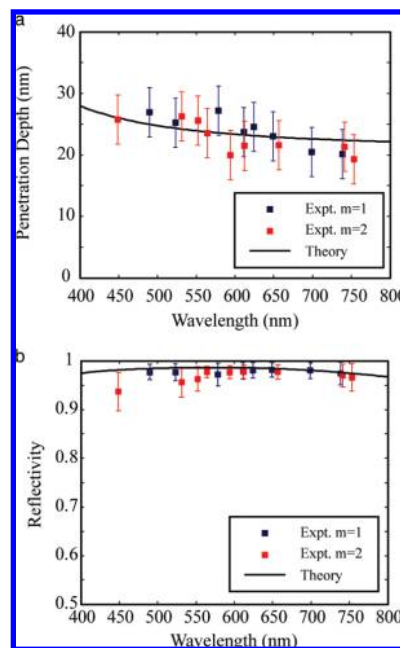

Figure 4. Characteristics of the nanocavity mirrors. (a) The penetration of SPPs into the cavity mirrors (square markers) compared with an approximate Fresnel reflection model[23] for SPPs (solid lines). The experimental penetration depth was calculated by comparing the measured resonant wavelength and physical cavity length. (b) The reflectivity (geometric average of both mirrors) of the nanocavity mirrors (square markers) compared with a phenomenological SPP reflection model (solid lines). The reflectivity is limited by intrinsic metal losses (at shorter wavelengths) and scattering due to the finite fin height (at longer wavelengths).

In conclusion, we have shown that chemical electroplating and controlled thin film metal deposition can yield high aspect ratio metal fins capable of efficient surface plasmon reflection. We showed that two closely spaced fins define a Fabry-Pérot nanocavity that concentrates surface plasmon polaritons at visible frequencies with a high Q-factor. Such high Q-factors are achievable when the cavity length is considerably shorter than the SPP propagation distance and the mirrors' heights are significantly larger than the SPP penetration depth into the air. A simple analytical model describes the observed results well when accounting for the surface plasmon dispersion and the effect of scattering and reflection from the metal fins. Concurrent high quality factors and subwavelength mode volumes would allow a strong Purcell effect competitive with higher Q-factor diffraction limited photonic crystal cavities and enables numerous applications[27] such as fast and efficient light emitting devices.[6,8,11]

Stefano Cabrini and Scott Dhuey for help with device fabrication. V.J.S. acknowledges a fellowship from the Intel Corporation.

References

(1) Maier, S. A. *Plasmonics, Fundamentals and Applications*; Springer: New York, 2007.
(2) Berini, P. *Phys. Rev. B* **2000**, *61*, 10484.
(3) Oulton, R. F.; Sorger, V. J.; Pile, D. F. P.; Genov, D. A.; Zhang, X. *Nat. Photonics* **2007**, *2*, 496–500.
(4) Ditlbacher, H.; Krenn, J. R.; Schider, G.; Leitner, A.; Aussenegg, F. R. *Appl. Phys. Lett.* **2002**, *81*, 1762–1764.
(5) (a) Pile, D. F. P.; Gramotnev, G. T. *App. Phys Lett.* **2005**, *86*, 161101. (b) Bozhevolnyi, S. I.; Volkov, V. S.; Devaux, E.; Laluet, J. -Y.; Ebbesen, T. W *Nature* **2006**, *440*, 508–511. (c) Steele, J. M.; Liu, Z. W.; Wang, Y.; Zhang, X. *Opt. Express* **2006**, *14*, 5664–5670. (d) Liu, Z. W.; Steele, J. M.; Lee, H.; Zhang, X. *Appl. Phys. Lett.* **2006**, *88*, 171108.
(6) Akimov, A. V.; Mukherjee, A.; Yu, C. L.; Chang, D. E.; Zibrov, A. S.; Hemmer, P. R.; Park, H.; Lukin, M. D. *Nature* **2007**, *450*, 402–406.
(7) (a) Miyazaki, H; Kurokawa, Y. *Phys. Rev. Lett.* **2006**, *96*, 097401. (b) Allione, M.; Temnov, V. V.; Fedutik, Y.; Woggon, U.; Artemyev, M. V. *Nano Lett.* **2008**, *8*, 31–35.
(8) Stoltz, N.; Rakher, M.; Strauf, S.; Badolato, A.; Lofgreen, D.; Petroff, P.; Coldren, L.; Bouwmeester, D. *Appl. Phys. Lett.* **2005**, *87*, 031105.
(9) Vahala, K. J. *Nature* **2003**, *424*, 839–846.
(10) Altug, H.; Englund, D.; Vuckovic, J. *Nature* **2006**, *2*, 484–488.
(11) Purcell, E. *Phys. Rev.* **1946**, *69*, 681.
(12) Bergman, D. I.; Stockman, M. I. *Phys. Rev. Lett.* **2003**, *90*, 027402.
(13) Yu, N.; Cubukcu, E.; Diehl, L.; Belkin, M. A.; Crozier, K. B.; Capasso, F.; Bour, D.; Corzine, S.; Höfler, G. *Appl. Phys. Lett.* **2007**, *91*, 173113.
(14) Baba, T.; Sano, D. *IEEE J. Sel. Top. Quantum Electron.* **2003**, *9*, 1340–1346.
(15) Lal, S.; Link, S.; Halas, N. J. *Nat. Photonics* **2007**, *1*, 641–648.
(16) Liu, Y.; Bartal, G.; Genov, D. A.; Zhang, X. *Phys. Rev. Lett.* **2007**, *99*, 153901.
(17) Hillenbrand, R.; Taubner, T.; Keilmann, F. *Nature* **2002**, *418*, 159–162.
(18) Min, B.; Ostby, E.; Sorger, V. J.; Ulin-Avila, E.; Yang, L.; Zhang, X.; Vahala, K. J. *Nature* **2009**, *457*, 455–458.
(19) Oulton, R. F.; Pile, D. F. P.; Liu, Y.; Zhang, X. *Phys. Rev. B* **2007**, *76*, 035408.
(20) Weeber, J.-C.; Bouhelier, A.; Colas de Francs, G.; Markey, L.; Dereux, A. *Nano Lett.* **2007**, *7*, 1352–1359.
(21) Oulton, R. F.; et al. *Opt. Commun.* **2001**, *195*, 327–338.
(22) Nguyen, P.; Zeng, Y.; Alford, T. L. *J. Vac. Sci. Technol., B* **1999**, *17*, 2204–2209.
(23) The dispersion relation, $k_{sp}(\lambda) = 2\pi n_{Ag}(\lambda)/\lambda[n_{Ag}(\lambda)^2 + 1]^{-1/2} = 2\pi n_{sp}(\lambda)/\lambda$ describes the propagation and attenuation characteristics of SPPs of the silver/air substrate interface, where the propagation distance is given by, $L_{sp} = \text{Im}\{2k_{sp}(\lambda)\}^{-1}$.
(24) Johnson, P. B.; Christie, R. W. Optical Constants of the Noble Metals. *Phys. Rev. B* **1972**, *6*, 4370.
(25) Palik, E. D. *Handbook of optical constants of solids*; Academic Press: New York, 1985.
(26) Elser, J.; Podolskiy, V. A. *Phys. Rev. Lett.* **2008**, *100*, 066402.
(27) Kirchain, R.; Kimerling, L. *Nat. Photonics* **2007**, *1*, 303–305.

NL901682N